Electrochemical Intercalation of Oxygen in La_2NiO_{4+x}: Phase Separation below Ambient Temperature

I. Yazdi, S. Bhavaraju, J. F. DiCarlo, D. P. Scarfe, and A. J. Jacobson*

Department of Chemistry and Texas Center for Superconductivity, University of Houston, Houston, Texas 77204-5641

Received May 10, 1994. Revised Manuscript Received August 5, 1994[⊗]

Electrochemical intercalation of oxygen in La_2NiO_{4+x} has been investigated by galvanostatic and potential step experiments for 268 K $\leq T \leq$ 295 K in the composition range $0 \leq x \leq 0.14$. At room temperature a single-phase region in the composition range ($0.06 < x < 0.14$) is observed. When the temperature is lowered to 273 K, the electrochemical data show evidence for phase separation into three distinct two-phase regions with compositions centered at $x = 0.076$, 0.100, and 0.119. Single-phase regions with compositions centered at $x = 0.065$, 0.087, and 0.112 are observed between the two-phase regions. The kinetics of the phase separation are slow. The results are consistent with recent low-temperature X-ray and neutron diffraction studies of phase separation at specific compositions.

Introduction

Intercalation of oxygen in oxides with the perovskite and La_2MO_4 (M = Cu, Ni) structures has recently been shown to occur at ambient temperature. Both chemical and electrochemical oxidation techniques in aqueous KOH electrolytes have been described.[1–19] The majority of the studies have examined the La_2CuO_{4+x} system because of the observation of superconductivity on oxidation.[1] Complex phase separation occurs as a function of composition and temperature, and two distinct superconducting compositions have been reported.[8,10] The phase separation and properties of the La_2CuO_4 system have recently been reviewed.[17] Similar experiments have been carried out on the structurally analogous La_2NiO_{4+x} phase.[9,11,14–16] The phase diagram of La_2NiO_{4+x} has also been extensively investigated by nonelectrochemical methods and like the copper system shows phase separation.[20–23]

Demourges et al. reported the synthesis of La_2NiO_{4+x} phases in the composition range $0 \leq x \leq 0.25$ by controlled potential electrolysis (600 mV vs Hg/HgO).[14] Specific compositions at $x = 0.0$, 0.03, 0.11, 0.14, 0.17, 0.18, 0.23, and 0.25 were synthesized and characterized by X-ray diffraction and by measurements of their open-circuit potentials. A neutron powder diffraction study of $La_2NiO_{4.25}$ prepared electrochemically[14] confirmed the location of the interstitial oxygen atoms in the La_2O_2 layers, in agreement with previous studies of oxidized samples prepared at high temperature.[20] Electron microscopy of $La_2NiO_{4.26}$ revealed the presence of a number of different commensurate and incommensurate superlattices associated with the interstitial oxygen distribution and content.[15]

DiCarlo et al.[16] examined electrochemical intercalation in La_2NiO_{4+x} at lower compositions, $0 \leq x \leq 0.145$, by galvanostatic and potential step methods. At ambient temperature the intercalation–deintercalation reactions were shown to be reversible, and the electrochemical data give direct information about the phase diagram. A single-phase region in the composition range $0.06 < x < 0.145$, a two-phase region for $0.01 < x \leq 0.06$, and a single-phase region for $0 \leq x < 0.01$ were observed. The results are in excellent agreement with those of Rice and Buttrey obtained by equilibration of La_2NiO_{4+x}

[⊗] Abstract published in *Advance ACS Abstracts,* September 15, 1994.

(1) Wattiaux, A.; Park, J.-C.; Grenier, J.-C.; Pouchard, M. *C. R. Acad. Sci. Paris, Ser. II*, **1990**, *310*, 1047.
(2) Suryanarayanan, R.; Gorochov, O.; Rao, M. S. R.; Ouhammou, L.; Paulus, W.; Heger, G. *Physica C* **1991**, *185–189*, 573.
(3) Grenier, J.-C.; Wattiaux, A.; Lagueyte, N.; Park, J.-C.; Marquestaut, E.; Etourneau, J.; Pouchard, M. *Physica C* **1991**, *173*, 139.
(4) Wattiaux, A.; Fournès, L. ; Demourges, A.; Bernaben, N.; Grenier, J.-C.; Pouchard, M. *Solid State Commun.* **1991**, *77*, 489.
(5) Bezdicka, P.; Wattiaux, A.; Grenier, J.-C.; Pouchard, M.; Hagenmuller, P. *Z. Anorg. Allg. Chem.* **1993**, *619*, 7.
(6) Rudolf, P.; Schöllhorn, R. *J. Chem. Soc., Chem. Commun.* **1992**, 1158.
(7) Rudolf, P.; Paulus, W.; Schöllhorn, R. *Adv. Mater.* **1991**, *3*, 438.
(8) Grenier, J.-C.; Lagueyte, N.; Wattiaux, A.; Doumerc, J.-P.; Dordor, P.; Etourneau, J.; Pouchard, M.; Goodenough, J. B.; Zhou, J. S. *Physica C* **1992**, *202*, 209.
(9) Grenier, J.-C.; Wattiaux, A.; Doumerc, J.-P.; Dordor, P.; Fournès, L.; Chaminade, J.-P.; Pouchard, M. *J. Solid State Chem.* **1992**, *96*, 20.
(10) Chou, F. C.; Cho, J. H.; Johnston, D. C. *Physica C* **1992**, *197*, 303.
(11) Grenier, J.-C.; Wattiaux, A.; Demourges, A.; Pouchard, M.; Hagenmuller, P. *Solid State Ionics* **1993**, *63–65*, 825.
(12) Radaelli, P. G.; Jorgensen, J. D.; Schultz, A. J.; Hunter, B. A.; Wagner, J. L.; Chou, F. C.; Johnston, D. C. *Phys. Rev. B* **1993**, *48*, 499.
(13) Takayama-Muromachi, E.; Sasaki, T.; Matsui, Y. *Physica C* **1993**, *207*, 97.
(14) Demourges, A.; Wattiaux, A.; Grenier, J.-C.; Pouchard, M.; Soubeyroux, J. L.; Dance, J. M.; Hagenmuller, P. *J. Solid State Chem.* **1993**, *105*, 458.
(15) Demourges, A.; Weill, F.; Grenier, J.-C.; Wattiaux, A.; Pouchard, M. *Physica C* **1992**, *192*, 425.
(16) DiCarlo, J. F.; Yazdi, I.; Bhavaraju, S.; Jacobson, A. J. *Chem. Mater.* **1993**, *5*, 1692.
(17) Johnston, D. C.; Borsa, F.; Canfield, P. C.; Cho, J. H.; Chou, F. C.; Miller, L. L.; Torgeson, D. R.; Vaknin, D.; Zarestky, J.; Ziolo, J.; Jorgensen, J. D.; Radaelli, P. G.; Schultz, A. J.; Wagner, J. L.; Cheong, S.-W.; Bayless, W. R.; Schirber, J. E.; Fisk, Z. *Proceedings of a Workshop on "Phase Separation in Cuprate Superconductors,"*: Coltbus, Germany 4–10 Sept. 1993 Springer-Verlag, to be published.
(18) Schwartz, M.; Cahen, D.; Rappaport, M.; Hodes, G. *Solid State Ionics* **1989**, *32/33*, 1137.
(19) Scolnik, J.; Rappaport, M.; Hass, N.; Dai, U.; Cahen, D. *Physica C* **1993**, *209*, 1993.
(20) Jorgensen, J. D.; Dabrowski, B.; Pei, S.; Richards, D. R.; Hinks, D. G. *Phys. Rev. B* **1989**, *40*, 2187.
(21) Rice, D. E.; Buttrey, D. J. *J. Solid State Chem.* **1993**, *105*, 197.
(22) Tamura, H.; Hayashi, A.; Ueda, Y. *Physica C* **1993**, *216*, 83.
(23) Buttrey, D. J.; Honig, J. M. In *The Chemistry of High Temperature Superconductors*, Rao, C. N. R., Ed.; World Scientific Publishing: Singapore, 1991; pp 283–305.

0897-4756/94/2806-2078$04.50/0

crystals in oxygen at higher temperatures.[21] The only discrepancy between the phase diagrams determined by the two methods is that a phase with $P4_2/ncm$ symmetry in the narrow composition range ($0.02 < x < 0.03$) was not observed in electrochemical experiments using polycrystalline electrodes.

Recent synchrotron X-ray and neutron diffraction measurements indicate that phase separation occurs in the single-phase composition region ($0.06 < x < 0.145$) on cooling to just below room temperature.[24,25] The initial study[24] suggested that $La_2NiO_{4.105}$ phase separates below room temperature into an orthorhombic phase with a doubled c axis and a tetragonal phase. A more detailed investigation of this and other compositions has subsequently provided a more detailed description of the phase diagram.[25] The neutron diffraction data were interpreted in terms of staged layers of intercalated oxygen atoms between La_2NiO_4 layers with the orthorhombic $Bmab$ type of distortion. The oxygen atoms occupy intestitial sites in the La_2O_2 layers. The phase at $x = 0.105$, for example, has been identified as a single-phase stage-2 material. In general, phase separations were observed to occur quite slowly and to show hysteresis.

The neutron diffraction studies[24,25] suggest that the phase separation should be apparent in electrochemical measurements at temperatures below ambient. In this paper, an electrochemical study of the phase diagram of La_2NiO_{4+x} at temperatures between 268 and 295 K is described and the results compared with the neutron diffraction measurements.

Experimental Section

La_2NiO_{4+x} was prepared by standard solid state techniques. Stoichiometric amounts of La_2O_3 (predried at 800 °C, Aldrich 99.9%) and NiO (Aldrich 99.99%) were ground and heated in air at temperatures of 1250 (24 h), 1250 (24 h), 1270 (48 h), and 1300 °C (12 h). The sample was pelletized and heated to 1380 °C for 12 h. Powder X-ray diffraction data were measured with a Scintag XDS2000 diffractometer using Cu Kα radiation in the range $10° \leq 2\Theta \leq 70°$. Measurements were made on the starting material and on electrodes. The electrodes were mounted directly on the diffractometer and diffraction patterns recorded from the front surface. Lattice constants were obtained by fitting the data using GSAS.[26] The starting electrode material was tetragonal ($I4/mmm$) with lattice constants a = 3.866(1) and c = 12.665(2) Å. At the end of the entire sequence of experiments (~3 months), an X-ray diffraction pattern of the electrode showed no lines due to impurity phases and little evidence for line broadening. Tetragonal lattice constants of a = 3.858(1) Å and c = 12.609(1) Å were obtained for a partially oxidized sample. The X-ray diffraction patterns for the starting material and final product are shown in Figure 1. Thermogravimetric measurements were performed by reduction of the sample to nickel metal and lanthanum oxide in a 5% hydrogen–95% nitrogen atmosphere to determine the oxygen content.

Samples prepared by the above procedure were used in the electrochemical experiments in the following way. A pellet, 75.70 mg and 8 mm in diameter, was painted on one surface with gold paste, and a 0.025 cm diameter platinum wire was attached to the paint. The gold film was then dried at room temperature for 3 h, annealed in air at 900 °C for 12 h, and

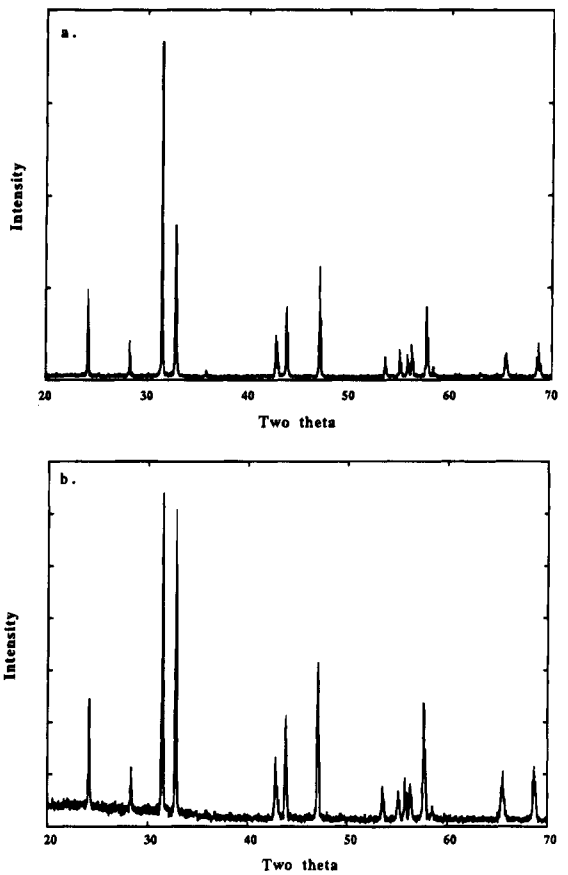

Figure 1. X-ray diffraction patterns of the La_2NiO_4 starting material and of the La_2NiO_4 electrode at the end of the low-temperature experiments.

furnace cooled. Leads attached by this method were shown to behave ohmically by placing two such gold films on either side of a pellet and checking the $I-V$ characteristics. A linear relationship between current and voltage indicated proper ohmic contact. Pellets without gold paint but heat treated in the same way were analyzed thermogravimetrically and had an average composition $La_2NiO_{4.13\pm0.02}$. The microstructures of typical electrodes were examined by scanning electron microscopy using an ISI SS40 instrument. A typical microstructure is shown in Figure 2 for the surface and for a cross section of an electrode. The La_2NiO_4 particle sizes are 5–10 μm.

Electrochemical experiments were performed using a Biologic MacPile potentiostat–galvanostat and a three-electrode system with the sample as the working electrode, gold foil as the counter electrode, and Hg/HgO/1 M KOH ($E_0 = +0.098$ V vs SHE) as the reference electrode. The electrolyte was 1 M KOH that had been purged with nitrogen for 3 h prior to the start of an experiment. The experiments were carried out with a continuous nitrogen purge to avoid the competing reaction of oxygen reduction that can occur at low potentials. The temperature of the cell was lowered in a bath of ethylene glycol and water, cooled by a cold-finger Neslab bath cooler. The reference electrode was at ambient temperature during the experiment. The temperature was maintained at the desired level (±0.2 °C) with a Therm-O-Watch L6.1000SS temperature controller and a mercury thermometer.

Results

Electrochemical reduction and reoxidation of La_2NiO_{4+x} were studied by both galvanostatic (constant current) and potential step techniques. Galvanostatic experiments provide an overview of the changes in the composition and kinetics occurring during the intercalation reaction. Potential step experiments[27] provide

(24) Tranquada, J. M.; Buttrey, D. J.; Rice, D. E. *Phys. Rev. Lett.* **1993**, *70*, 445.
(25) Tranquada, J. M.; Kong, Y.; Lorenzo, J. E.; Buttrey, D. J.; Rice, D. E.; Sachan, V. *Phys. Rev. B*, in press.
(26) von Dreele, R. B.; Larson, A. C. *GSAS Users Guide*; Los Alamos National Laboratory: Los Alamos, NM, 1985-1992GSAS.

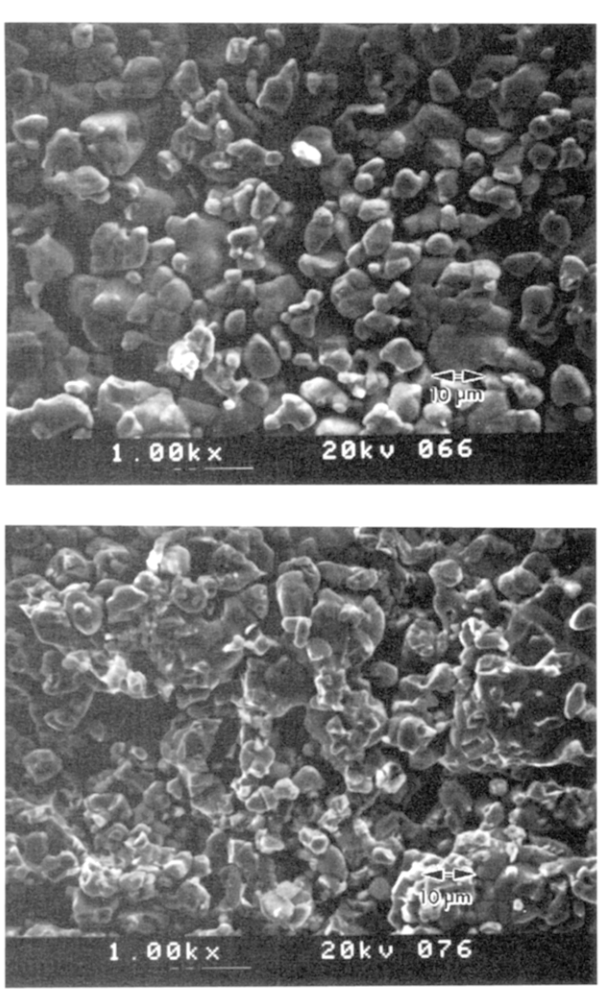

Figure 2. Scanning electron micrographs of (a) the top surface and (b) a cross section of a La_2NiO_4 electrode.

more details of the intercalation chemistry. In potential step experiments, the potential is changed abruptly by a small amount from the equilibrium value, and the current is monitored. The voltage step away from equilibrium initially produces a large current which then decays to a small preset value. When the current falls to the preset limiting current value, the voltage is stepped again. With small voltage steps, the potential step technique provides high composition resolution and data approaching, but not at, true equilibrium. The approach to equilibrium is determined by the value of the limiting current. Data are acquired rapidly because on each step the initial current is high. A galvanostatic experiment carried out at the limiting current would take much longer. True open-circuit (equilibrium) measurements are even slower and consequently cannot be used to obtain data for many different compositions. The potential step approach is a compromise technique that provides "quasi-equilibrium" data with high composition resolution.

Equilibrium data can be used to determine the number of phases present in specific composition ranges for the pseudobinary system La_2NiO_{4+x}. The approach has been well documented for a wide range of intercalation systems.[28] Problems with the interpretation can

(27) Thompson, A. H. *J. Electrochem. Soc.* **1979**, *126*, 603.
(28) Armand, M. In *Materials for Advanced Batteries*; Murphy, D. W., Broadhead, J., Steele, B. C. H., Eds.; Plenum: New York, 1980; p 145.

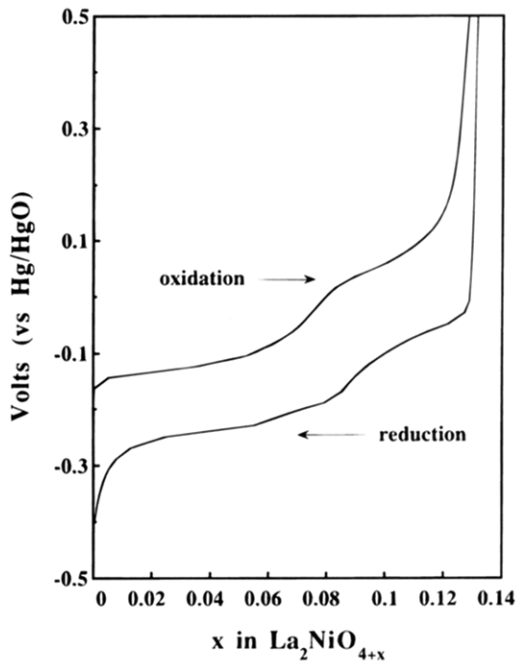

Figure 3. Galvanostatic reduction and oxidation curves (50 μA) for La_2NiO_4 at 273 K.

arise from nonequilibrium effects particularly when the free energy differences between adjacent phases are very small. In the present experiments, a small limiting current was used (10 μA) and uncertainties due to nonequilibrium effects were assessed by measurements made on both oxidation and reduction cycles. All of the features seen in reduction are also observed on oxidation. The effect of using a finite limiting current shows up only as a relative offset in V and x of the reduction and oxidation data.

Galvanostatic Measurements. Galvanostatic measurements were made at a constant current of 50 μA (100 $\mu A/cm^2$) between the voltage limits of -0.4 and $+0.6$ V versus Hg/HgO. Each time the temperature was changed the sample was reduced to a voltage cutoff of -0.5 V in order to obtain a stoichiometry as close as possible to $La_2NiO_{4.0}$. Measurements were made in the following temperature sequence: 273, 283, 295, and 268 K.

The galvanostatic data at 273 K are shown in Figure 3 for one complete oxidation and reduction cycle. The data show that the oxidation–reduction reaction is reversible with respect to the change in the composition and there is no indication of O_2 evolution on oxidation. The two-phase region observed at room temperature[16] in the composition range $0.01 \leq x \leq 0.06$ is also apparent in the data at 273 K. The separation in voltage between the oxidation and reduction cycle at $x = 0.03$ is 0.12 V. A new plateau region indicating two phase behavior is observed at 273 K on oxidation between $x = 0.08$ and 0.12. The same feature is observed in the reduction cycle but is offset in composition. At room temperature a single phase is observed in this composition range. The polarization measured by the difference in voltage between the oxidation and reduction cycles is higher in this region ($\Delta V = 0.16$ at $x = 0.11$) than in the range $0.01 \leq x \leq 0.06$. The transition region between the two two-phase regions is complex and different between oxidation and reduction cycles. Clearly the reaction is far from equilibrium at these current densities (100 $\mu A/cm^2$).

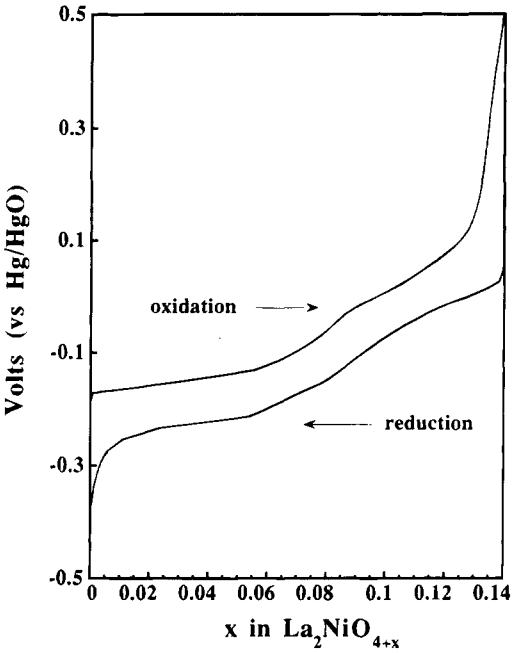

Figure 4. Galvanostatic reduction and oxidation curves (50 μA) for La_2NiO_4 at 283 K.

The galvanostatic results at 283 K are essentially similar (Figure 4), though the data are significantly less polarized ($\Delta V = 0.086$ at $x = 0.03$ and $\Delta V = 0.089$ at $x = 0.11$). More than one change in slope is apparent between the low and high composition regions suggesting the possibility of more than one intermediate phase. When the temperature is lowered to 268 K, the polarization increases significantly and the galvanostatic data are no longer reversible in that the oxygen removed on reduction cannot quantitatively be reintercalated on oxidation.

When the temperature is lowered from 295 to 268 K, the maximum composition that can be reached on oxidation decreases. The overpotential for O_2 evolution also decreased as the experiments proceeded and consequently, the compositions measured at the upper cutoff voltage of 0.6 V are overestimates of the amount of intercalated oxygen. Values of x at 0.4 V ($x = 0.148$ at 295 K, 0.137 at 283 K, 0.127 at 273 K, and 0.116 at 268 K), well below oxygen evolution, are not sensitive to this effect and show the progression with temperature in the maximum composition that can be obtained on oxidation. The oxidation curves for the data at the four temperatures are shown in Figure 5. The differences in the maximum oxygen content that can be obtained at the different temperatures are probably due to the slower kinetics at lower temperatures. It is also possible that the phase boundary at the high oxygen contents is strongly temperature dependent.

Potential Step Experiments. Potential step experiments were carried out at 273 and 283 K on the same sample used for the galvanostatic experiments. These results will be compared with the data taken at 295 K on a separate electrode from the same batch of starting materials. The experiments used 5 mV steps in the voltage with a lower current cutoff of 10 μA. The ambient temperature data are shown in Figure 6 for reduction (top) and oxidation (bottom). The reduction data were reported previously.[16] The derivative of the composition with respect to voltage (dx/dV) is also

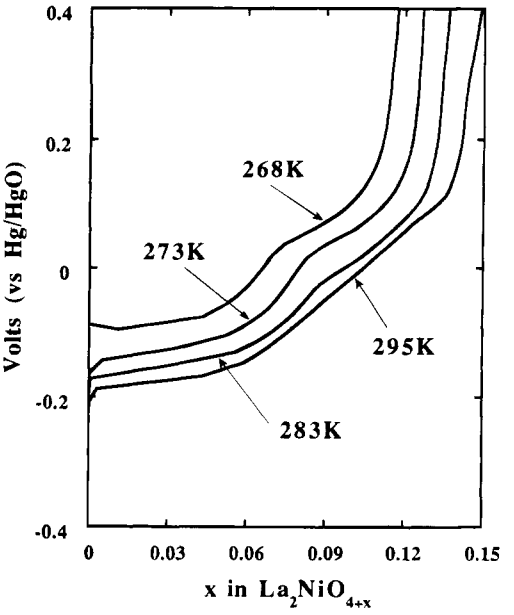

Figure 5. Galvanostatic oxidation data for La_2NiO_4 at 268, 273, 283, and 295 K.

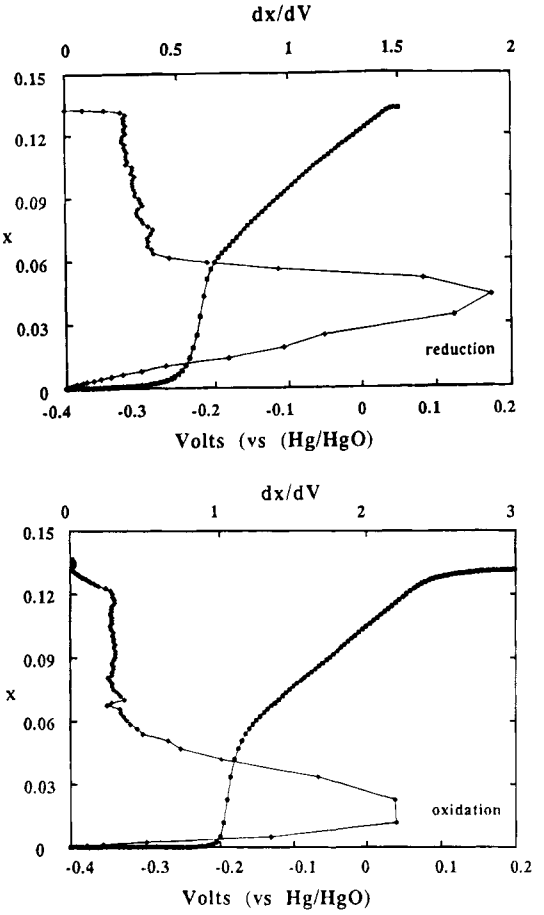

Figure 6. Variation of voltage with composition (x) for reduction and oxidation of La_2NiO_{4+x} at 295 K obtained from potential step data. The reduction and oxidation data are shown in the top and bottom panels, respectively. In each case, peaks in the derivative (dx/dV) correspond to the centers of two phase regions.

shown. The derivative plot is useful in locating intermediate phases. Ideally, maxima in dx/dV correspond to the midpoints in composition of two-phase regions. In practice, because of kinetic effects associated with diffusion and nucleation, the curves are broadened and

Table 1. Summary of the Voltage and Composition Data Obtained from the Potential Step Measurements at 273 and 283 K

		oxidation				reduction				average			
273 K	x at $(dx/dV)_{max}$	0.045	0.082	0.106	0.123	0.018	0.070	0.094	0.115	0.032	0.076	0.100	0.119
	V	−0.160	−0.110	0.000	+0.050	−0.210	−0.170	−0.060	−0.015	−0.185	−0.140	0.030	0.018
	x at $(dV/dx)_{max}$		0.064	0.081	0.112		0.065	0.093	0.111		0.065	0.087	0.112
	V		−0.124	−0.051	−0.037		−0.187	−0.124	−0.046		−0.156	−0.088	−0.005
283 K	x at $(dx/dV)_{max}$	0.008	0.072	0.092	0.116	0.05	0.081	0.105	0.127	0.029	0.077	0.099	0.122
	V	−0.186	−0.171	−0.036	0.037	−0.206	−0.140	−0.047	0.012	−0.196	−0.156	−0.042	0.025
	x at $(dV/dx)_{max}$		0.067	0.083	0.110		0.067	0.091	0.110		0.067	0.087	0.11
	V		−0.131	−0.076	0.016		−0.176	−0.105	−0.030		−0.154	−0.091	−0.007

shifted in position between the oxidation and reduction cycles.

The ambient temperature data are consistent with the phase diagram reported by Rice and Buttrey.[24] A single phase exists in the composition range from $x = 0.06$ to the upper composition limit that can be accessed before oxygen evolution occurs ($x = 0.14-0.15$). The single-phase region is characterized by a nearly constant value for dx/dV. Below $x = 0.06$, a two phase region is indicated by a nearly constant voltage and a maximum in dx/dV. The compositions at the derivative peak maxima are 0.025 and 0.047 for the reduction and oxidation data, respectively. The average value is 0.036, slightly higher than the expected composition midpoint from the published equilibrium phase diagram. Exact correspondence of the average midpoint and the equilibrium midpoint requires that polarization effects are equal in each direction. In general, the pathway will contribute some difference to the kinetics and an exact average is not expected. A single phase with space group $P4_2/ncm$ and $x = 0.03$ reported by Rice and Buttrey[21] is not observed in the present experiments using polycrystalline samples. The $P4_2/ncm$ phase has been observed in electrochemical experiments with a single crystal of La_2NiO_4 and shown to exist only over a narrow range of composition.[29] The formation of this phase may play a role in the reaction kinetics in the two phase region below $x = 0.06$, even though it is not directly observed in data for polycrystalline electrodes.

Data were collected at 273 K for two complete cycles of oxidation and reduction after an initial reduction to fix the starting composition at $x = 0$. The data for the two complete cycles of oxidation and reduction were nearly identical. Data for the second oxidation and third reduction are shown together in Figure 7. The third reduction cycle data together with the derivative dx/dV are shown in Figure 8 on an expanded scale. The oxidation and reduction data are shown in Figure 9 in the same format for comparison with the 295 K results in Figure 6. In addition to the maximum in the derivative corresponding to the two-phase region below $x = 0.06$, three peaks in dx/dV are observed in the composition region that is single phase at 295 K (Figure 8). The maxima are observed in both oxidation and reduction but are more pronounced in the reduction data. Values of x and V corresponding to the maxima on oxidation and reduction, and the average values are given in Table 1.

In a similar way, maxima in the derivative dV/dx can be used to locate the composition centers of the single phases between the two-phase regions. These data are not shown graphically, but values of x and V corresponding to the dV/dx maxima are given in Table I. The data show that the single-phase region at 295 K

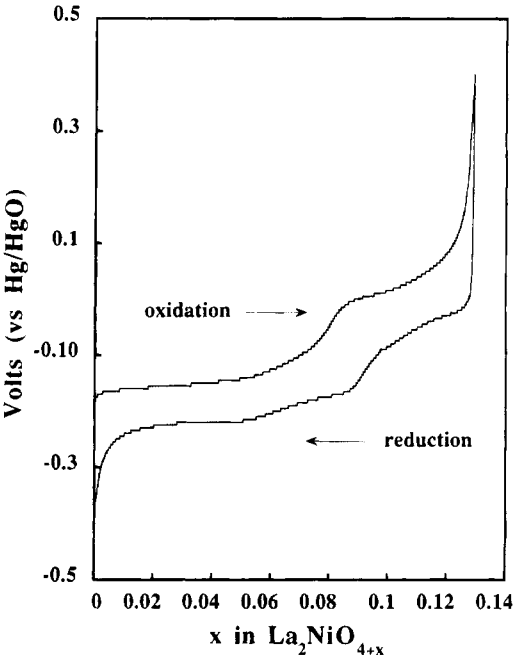

Figure 7. Variation of voltage with composition for the second oxidation and the third reduction of La_2NiO_{4+x} at 273 K obtained from potential step data.

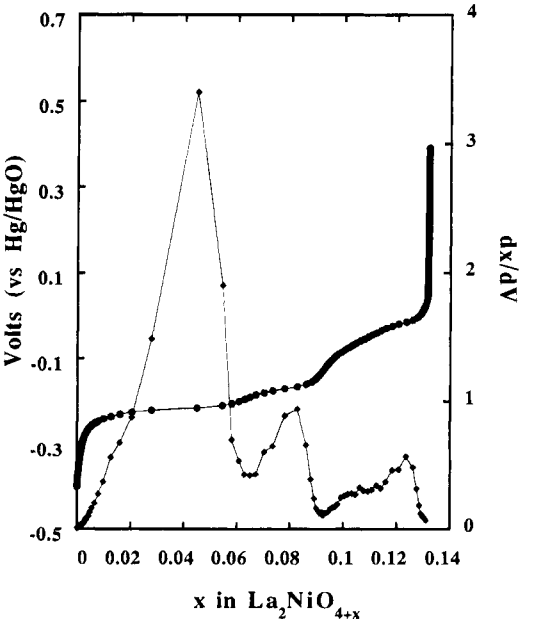

Figure 8. Variation of voltage with composition for the third reduction cycle reduction of La_2NiO_{4+x} at 273 K obtained from potential step data. Peaks in the derivative (dx/dV) correspond to the centers of two-phase regions.

(29) DiCarlo, J. F.; Yazdi, I.; Bhavaraju, S.; Jacobson, A. J.; Buttrey, D. J., to be published.

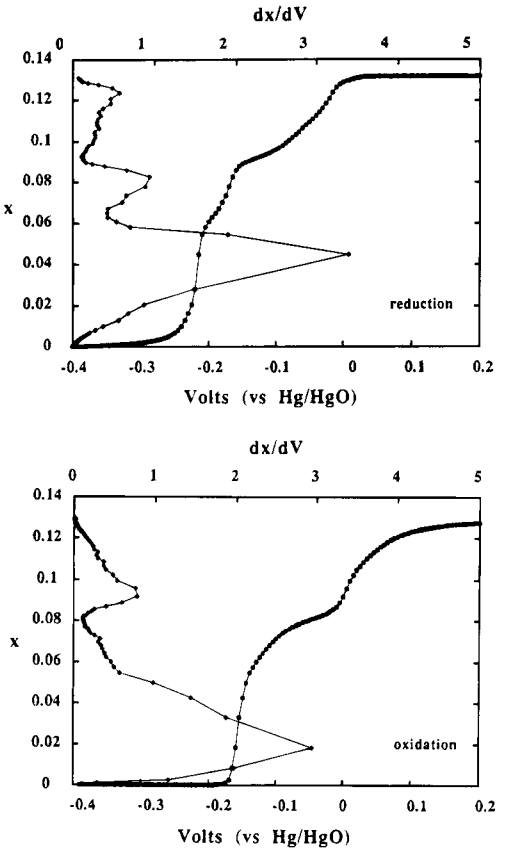

Figure 9. Variation of voltage with composition (x) for reduction and oxidation of La_2NiO_{4+x} at 273 K obtained from potential step data. The reduction and oxidation data are shown in the top and bottom panels, respectively. In each case, peaks in the derivative (dx/dV) correspond to the centers of two phase regions.

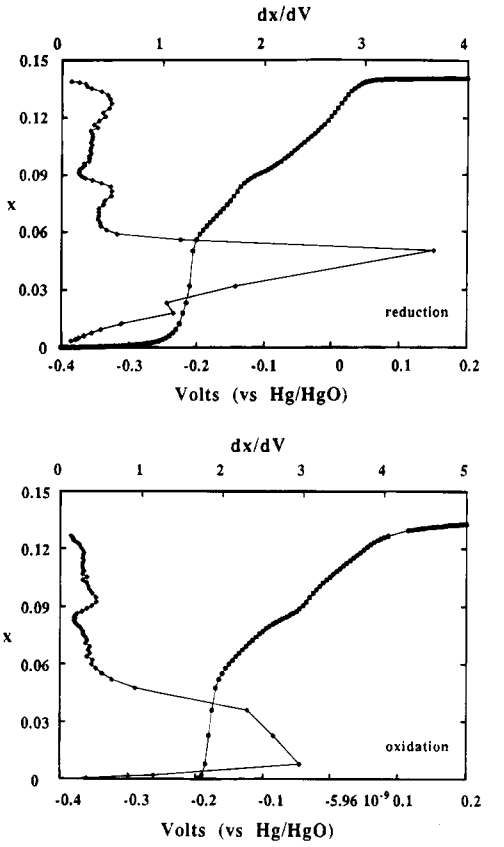

Figure 10. Variation of voltage with composition (x) for reduction and oxidation of La_2NiO_{4+x} at 283 K obtained from potential step data. The reduction and oxidation data are shown in the top and bottom panels, respectively. In each case peaks in the derivative (dx/dV) correspond to the centers of two phase regions.

separates into three two-phase regions with midpoint compositions corresponding to $x = 0.08$, 0.10, and 0.12.

The resolution in these experiments is insufficient to more precisely define the phase boundaries. Open-circuit voltage measurements at specific compositions are required to complete the phase diagram. The present data combined with the additional information provided by structural measurements enables the selection of a minimum set of compositions to further define the phase diagram. It should be noted, however, that the equilibration times needed to obtain open-circuit voltages are expected to be long. The present "quasi-equilibrium" experiments typically took 11 days for one complete cycle of reduction and oxidation.

Similar potential step data were also measured at 283 K and are shown in Figure 10. Values of x and V corresponding to the maxima on oxidation and reduction and the average values are given in Table 1. Qualitatively the data at 283 and 273 K are similar (Figures 9 and 10) though the derivative peaks are not quite so sharp in the 283 K data. A more quantitative comparison can be made using the results in Table 1. The average compositions at which the maxima in both dx/dV and dV/dx occur are closely similar indicating that the phase diagram is little altered in cooling from 283 to 273 K.

Discussion

Electrochemical intercalation and deintercalation experiments on La_2NiO_4 below ambient temperature indicate that phase separation occurs in the composition range $0.06 \leq x \leq 0.14$. The phase separation is indicated by the appearance of a plateau in galvanostatic data when the fully reduced composition is oxidized. The plateau is clearly apparent at 283 K and becomes even more pronounced at lower temperatures.

When the temperature is lowered, the cell resistance increases and the intercalation rates decrease. A combination of the two effects limits the lowest temperature at which useful data can be obtained to 273 K. Below this temperature composition changes are not reversible between oxidation and reduction cycles.

Potential step experiments provide more detail on the phase separation behavior for $0.06 \leq x \leq 0.14$. The kinetics are slow relative to the phase separation observed in the composition range $0 \leq x \leq 0.06$. The slower kinetics are indicated by the composition differences between corresponding peaks observed on oxidation and reduction cycles and are indicative of a complex structural reorganization. The data at 283 and 273 K are essentially the same. Maxima in the derivatives dx/dV and dV/dx have been used to obtain compositions corresponding to the centers of the two-phase and the single-phase regions, respectively. The average values obtained for the oxidation and reduction cycles provide a good approximation to the equilibrium phase diagram assuming that the magnitude of the polarizations due to the reaction kinetics are the same on the oxidation and reduction cycles.

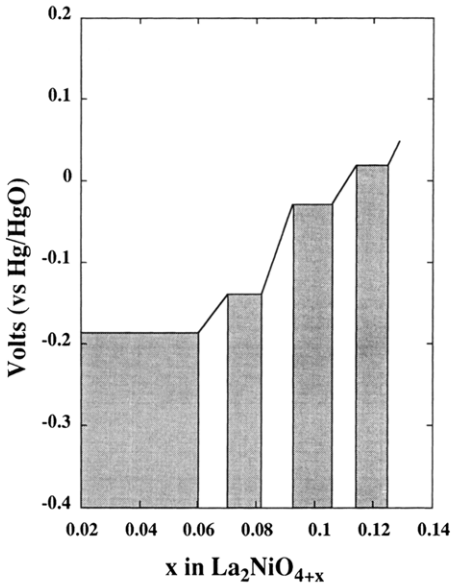

Figure 11. Schematic phase diagram for La_2NiO_{4+x} at 273 K; the shaded areas indicate two-phase regions.

The derivative plots show in Figures 9 and 10 show well-defined though broad maxima that are shifted in composition between the oxidation and reduction cycles. The number of peaks is the same for both cycles and the correspondence between the peaks in the oxidation and reduction data is clear. The width of the derivative peaks suggests that further resolution might be possible in even slower experiments.

On the basis of the data in Table 1, a schematic phase diagram can be constructed. The exact phase boundaries are uncertain and have been estimated from the widths of the maxima in dx/dV. The results obtained by analysis of the 273 and 283 K data are almost identical. The schematic phase diagram is shown in Figure 11. The single-phase region observed at ambient temperature separates at 273 K into three two-phase regions with compositions centered at $x = 0.076$, 0.100, and 0.119. Single phases with compositions centered at $x = 0.065$, 0.087, and 0.112 separate the two-phase regions.

We have shown previously that the electrochemically determined phase diagram is closely similar to the ambient temperature phase diagram determined using diffraction studies of crystals with different compositions.[21] The different oxygen stoichiometries were prepared by annealing the crystals in different oxygen fugacities at high temperatures. The electrochemical results below ambient temperature also can be compared with the recent neutron diffraction studies on single crystals of La_2NiO_{4+x} with oxygen stoichiometries where $x = 0.105$, 0.085, 0.074, 0.06, and 0.058. Very detailed diffraction studies of the phases present and of the kinetics of phase separation as a function of temperature have been reported.[25] The data were interpreted in terms of the formation of staged compositions where layers containing interstitial oxygen atoms regularly alternate with specific numbers of empty layers. The staging is apparently similar to that observed in graphite and the layered dichacogenides. A stange n compound has one filled layer regularly ordered with $n - 1$ empty layers. The phase diagram determined by the neutron diffraction studies for the La_2NiO_{4+x} system below ambient temperature can be compared with the electrochemical data. For $x \leq 0.06$ the electrochemical data and the structural measurements show that the phase diagram is unaltered on cooling. The electrochemical data on polycrystalline electrode do not show the $P4_2/ncm$ phase though it has been observed in recent single-crystal electrochemical measurements.[29] For $x \geq 0.06$, the neutron diffraction data indicate phase separation into two phases: a stage 3 compound with $0.065 \leq x \leq 0.70$; and a stage 2 compound with $0.10 \leq x \leq 0.11$. These two phases correspond to the two single-phase regions determined from the electrochemical data with compositions centered at 0.065 and 0.11. The agreement is very close though not exact due to uncertainties in determining the boundaries in each experiment. In the electrochemical data, uncertainties in phase boundaries arise from the broadening of the data due to non-equilibrium effects. The phase limits determined structurally are limited by the number of measured compositions. Taking these factors into account, the agreement is very good. The electrochemical data also indicate the formation of a distinct phase with a composition centered at $x = 0.087$, not identified in the neutron diffraction study. The structural phase diagram proposed by Tranquada et al.[25] suggests that this composition should lie in a two-phase region, but compositions close to this value were not examined in the neutron diffraction experiments (the nearest were 0.085 and 0.105). Some evidence for the existence of a distinct phase at $x = 0.09$ has been obtained by synchrotron X-ray diffraction.[30] The electrochemical data indicate that further structural studies $x = 0.087$ would be of value to determine the nature of this phase.

Initial studies at ambient temperature show that more detailed information can be obtained by using single-crystal electrodes. Electrochemical experiments currently in progress on single crystals at lower temperatures are expected to provide more information on the precise location of the phase boundaries.

Electrochemical intercalation provides very high composition resolution but only over a limited range of temperature. In contrast, the structural studies provide great detail over a wide range of temperature but at specific compositions. The two techniques provide complementary information and together can be used to map out the detailed phase equilibria in oxide systems like La_2NiO_4 that have remarkably high oxygen diffusivities.

Acknowledgment. We thank D. J. Buttrey for helpful discussions. The work was supported in part by the Robert A. Welch foundation (Grant No. 1207).

(30) Buttrey, D. J.; Rice, D. E., to be published.